



HAL
open science

New insights of butadiene production from ethanol: Elucidation of concurrent reaction pathways and kinetic study

Damien Dussol, Nicolas Cadran, Nicolas Laloue, Laurent Renaudot,
Jean-Marc Schweitzer

► To cite this version:

Damien Dussol, Nicolas Cadran, Nicolas Laloue, Laurent Renaudot, Jean-Marc Schweitzer. New insights of butadiene production from ethanol: Elucidation of concurrent reaction pathways and kinetic study. *Chemical Engineering Journal*, 2020, 391, pp.123586. 10.1016/j.cej.2019.123586 . hal-03118043

HAL Id: hal-03118043

<https://ifp.hal.science/hal-03118043>

Submitted on 4 Feb 2021

HAL is a multi-disciplinary open access archive for the deposit and dissemination of scientific research documents, whether they are published or not. The documents may come from teaching and research institutions in France or abroad, or from public or private research centers.

L'archive ouverte pluridisciplinaire **HAL**, est destinée au dépôt et à la diffusion de documents scientifiques de niveau recherche, publiés ou non, émanant des établissements d'enseignement et de recherche français ou étrangers, des laboratoires publics ou privés.

New insights of Butadiene production from Ethanol: elucidation of concurrent reaction pathways and kinetic study

D. Dussol, N. Cadran, N. Laloue*, L. Renaudot, J.-M. Schweitzer

IFP Energies nouvelles, Rond-point de l'échangeur de Solaize, 69360 Solaize, France

**Corresponding author: nicolas.laloue@ifpen.fr*

Abstract

While most papers focus on catalysts improvement, this paper is about a kinetic model based on a new reaction scheme to explain the transformation of ethanol/acetaldehyde to butadiene and side products. The reaction scheme presented here is more complex than the route usually presented in the literature, i.e. Gorin-Jones route. In order to develop this kinetic model, the reaction scheme is studied by means of fixed bed type catalytic tests using Ta₂O₅-SiO₂ catalysts with a temperature range from 320 °C to 370 °C and a constant pressure. The reactor (gas / solid, isothermal and isobaric) is modelled in steady state. It is concluded that the model that includes two different routes of butadiene production is in good agreement with the productions of major products and is necessary to explain the formation of some side products, highlighting a brand new reaction scheme for ethanol-to-butadiene transformation.

Keywords: 1,3-Butadiene, Ethanol, Kinetics, Reaction scheme, Tantalum oxide

Nomenclature

SI Units

| | |
|------------|--------------------------------------|
| C^g | Gas concentration |
| D_{ax} | Axial dispersion coefficient |
| D_e | Molecular diffusivity |
| D_M | Molecular diffusion coefficient |
| d_p | Particle diameter |
| E_a | Activation energy |
| $f_{i,ex}$ | External resistance fraction |
| k | Kinetics constant |
| k° | Arrhenius law pre-exponential factor |
| K_{eq} | Equilibrium constant |

| | |
|------------------|--|
| k_{gs}° | External mass transfer standard coefficient ($m \cdot s^{-1}$) |
| L | Characteristic length ($=V_p/S_p$) |
| \dot{m}_c | Carbon mass flow |
| r | Reaction kinetics ($mol \cdot s^{-1} \cdot kg_{cata}^{-1}$) |
| \bar{r} | Apparent reaction kinetics ($mol \cdot s^{-1} \cdot kg_{cata}^{-1}$) |
| R | Gas constant |
| R_i | Production flow ($mol \cdot s^{-1} \cdot kg_{cata}^{-1}$) |
| Re | Reynolds number |
| S | Selectivity |
| Sc | Schmidt number |
| Sh | Sherwood number |
| S_p | Particle surface |
| t | Time |
| T | Temperature |
| u_v | fluid velocity in empty reactor |
| V_p | Particule volume |
| X | Conversion |
| z | Axial abscissa |
| β_p | Particle porosity |
| ε_g | Gas fraction of the bed |
| ε_s | Pores fraction of the bed ($=1 - \varepsilon_g$) |
| v | Stoichiometric coefficient |
| ρ_s | Particule density ($kg_{cata} \cdot m_{cata}^{-3}$) |
| φ_{su} | Weisz-Prater criterion |
| τ_p | Particle tortuosity |

1. Introduction

1,3-butadiene (BD) is a monomer used for the synthesis of polymers such as polybutadiene, styrene-butadiene and acrylonitrile butadiene styrene. With a global market over 12 million tons per year and a commercial price between 1,845 and 2,225€/t over the period 2008/2011, butadiene is a major product for industrial purposes [1]. Its use in the synthesis of many kinds of polymers makes it a product of primary importance for chemistry, especially for the production of synthetic rubber being therefore a critical product for the tyre industry [2]. Moreover the butadiene demand is in constant growth for strongly growing markets such as China and India [3]. Butadiene is mainly produced from steam cracking of paraffinic hydrocarbons. However other industrial processes for butadiene synthesis have been developed such as catalytic dehydrogenation of butane and butenes, and oxidative dehydrogenation of butenes [2]. Other ways of producing butadiene have been identified through the Reppe method involving acetylene and formaldehyde [4] or through the transformation of ethanol [5]. Recent economic studies on the bioethanol path exhibit substantial advantages in terms of economy and sustainability [3].

These perspectives combined with the fossil fuels depletion have made ethanol into butadiene process a suitable process for industrial use [6].

Two processes have been developed: the Lebedev process in one reactor and the Ostromislenky process in two reactors [7] both involving the same chemical route from ethanol to butadiene. The first step is the partial dehydrogenation of ethanol into acetaldehyde which occurs in the first reactor in the Ostromislenky process. The obtained ethanol (EtOH) and acetaldehyde (AcH) mixture gives butadiene after several successive chemical steps (see Figure 1).

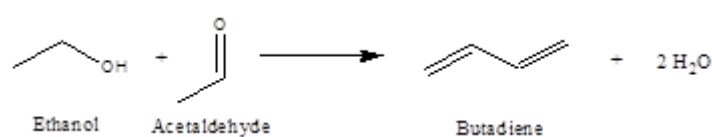


Figure 1 Overall stoichiometric reaction

The main catalysts studied for the Lebedev process are MgO/SiO₂ or M/Mox/SiO₂ where M is a metal (Ag, Cu...) mainly used for the dehydrogenation step and Mox is a metal oxide useful for the conversion of the EtOH/AcH mixture [8]. Transitional elements of Groups IV and V are in general the most selective catalysts [9]. In the case of the Ostromislenky process, M and Mox are present in the first and second reactor respectively. Tantalum oxide over silica (0.8 to 2.5% Ta₂O₅-SiO₂) seems to be especially efficient [10,11] and have been used

as industrial catalyst in the second reactor. The maximal selectivity is reached for an EtOH/AcH ratio around 3, *i.e.* with a large excess of ethanol [12]. The presence of water improves BD selectivity by reducing the formation of C6+ compounds [13]. Nowadays operating conditions are still studied to increase the performances [14,15].

Several reaction mechanisms studies have been realized although a total agreement was never reached within the scientific community [16]. Moreover there are very few studies focusing on the Ostromislensky second step reaction [17]. This study is an attempt to fulfill this lack.

This kinetic model based on a literature survey takes into account the transformation of an ethanol/acetaldehyde mixture into butadiene and major side products formation. The implemented kinetic laws for each reaction are order-based laws. The parameters optimisation will be performed over one set of experiments. Another set of experimental results is used to be compared with the kinetics modelling results in order to validate the accuracy of both the reaction scheme and the kinetic laws.

2. Experimental

2.1 Catalyst synthesis and pre-treatment

The catalyst support is silica gel SiO₂ (Davisil Grade 636), from Sigma-Aldrich with pore size of 60 Å and particle size of 35-60 mesh. Its apparent density is 0.53 g/cc and its pore porosity β_p is 0.8 g/cc. The chosen active phase Mox is Ta₂O₅. The 2:98 Ta₂O₅-SiO₂ was prepared by wetness impregnation of an alcoholic solution of Ta(OEt)₅ purchased from Sigma-Aldrich followed by a calcination step at 550 °C.

2.2 Catalytic test

The catalytic tests have been performed in a stainless steel fixed bed reactor. The amount of catalyst was 0.25 g. It is diluted in carborundum, an inert solid ($vol_{cata}/vol_{bed} = 10\%$). In agreement with the literature [12], the process temperature is 320 to 370 °C under a total pressure of 3 bar. Ethanol, water (18% mass) and acetaldehyde are injected with a liquid pump and vaporised in a stream of N₂ ($N_2/\{EtOH+AcH\}=1$ (mol/mol)). Two EtOH/AcH ratios are tested - 2.5 and 3.6 – to frame the optimal ratio of 3. The model parameters have been estimated using the ratio 3.6 data and then validated on ratio 2.5 data. Different conversions were obtained by using different flows. The Weight Hourly Space Velocity (WHSV) is based on the sum of EtOH and AcH mass flows and ranges from 1.1 to 8 g·g_{cat}⁻¹·h⁻¹. Reaction products are analysed by online gas chromatography (6890N

GC Agilent) with PONA column (20 m x 100 μm). They are performed after 24h on stream. The conversions are calculated with the carbon mass flows as defined below:

$$X_{ethanol} = 1 - \frac{\dot{m}_{c,EtOH}^{outlet}}{\dot{m}_{c,EtOH}^{inlet}} \quad (1)$$

$$X_{acetaldehyde} = 1 - \frac{\dot{m}_{c,AcH}^{outlet}}{\dot{m}_{c,AcH}^{inlet}} \quad (2)$$

The yield of each component is calculated as follow:

$$Y = 1 - \frac{\dot{m}_c^{outlet}}{\dot{m}_{c,EtOH}^{inlet} - \dot{m}_{c,AcH}^{inlet} - \dot{m}_{c,EtOH}^{outlet} - \dot{m}_{c,AcH}^{outlet}} \quad (3)$$

3. Theory and calculations

3.1 Reactor model

The lab scale fixed bed reactor device has been modelled to EtOH and AcH mixture transformation to BD. A reactor model was developed considering a two-phase (gas-solid) fixed bed system operating under isothermal conditions.

Material balances were written for each compound in the gas phase only since no diffusion limitation is generally expected with 200-500 μm ground catalysts. This assumption was a posteriori validated using diffusion limitation criteria (see section 3.2). A dispersed plug flow model for the gas flow has been considered to take into account potential back-mixing effect. The transient gas material balance for each component is given by equation (4).

$$\frac{\partial C^g}{\partial t} = \frac{1}{(\varepsilon_g + \varepsilon_p \cdot \varepsilon_s)} \left(\rho_s \varepsilon_s \sum_j v_j r_j - \frac{\partial(u_v C^g)}{\partial z} + D_{ax} \frac{\partial \varepsilon_g \partial C^g}{\partial z^2} \right) \quad (4)$$

Limit conditions: $C^g|_{z=0} = C_{inlet}^g$

$$D_{ax} \frac{\partial C^g}{\partial z} \Big|_{outlet} = 0$$

Moreover, in order to respect the equation of state (5) (ideal gas law assumption), the equation (6) that allows the gas velocity calculation has to be satisfied. It has been obtained by summing all the gas equations and introducing the equation of state (5).

$$\sum C_i^g = \frac{P_t}{RT_g} \quad (5)$$

$$\frac{\partial(u_v P_t)}{\partial z} = D_{ax} \frac{\partial}{\partial z} \left(\varepsilon_g \frac{\partial P_t}{\partial z} \right) + RT_g \rho_s \varepsilon_s \sum_i \sum_j v_{ij} r_j \quad (6)$$

The time integration of the obtained system of ordinary differential equations has been achieved by the LSODE solver [18] in order to reach the steady-state regime. A spatial discretization of the partial derivative equations has been performed using upwind and centered finite differences for convection and dispersion terms respectively [12].

3.2 Evaluation of eventual external and internal diffusion limitation

External diffusion limitation has been assessed using the external resistance fraction (f_{ex}) estimation (see equation (7)).

$$f_{ex} = \frac{|\sum_j \bar{F}_j| L}{\rho_s k_{gs}^\circ C_{ex}} \quad (7)$$

The external mass transfer coefficient $k_{gs,i}^\circ$ has been determined using the Kunii & Levenspiel correlation [19] (see equation (8)).

$$Sh = 2 + 1.8 * Re^{1/2} * Sc^{1/3} \quad (8)$$

$$\text{with } Sh = \frac{k_{gs}^\circ d_p}{D_M} \quad (9)$$

The molecular diffusion coefficient D_M has been calculated using the Fuller method (1966) [20].

The external resistance fraction being less than 5 % for each component, the absence of external transfer limitation has been confirmed.

Internal diffusion limitations have been evaluated through the Weisz-Prater criterion assessment [21].

$$\Phi_{su} = \frac{|\sum_j \bar{F}_j| L^2}{\rho_s D_e C_{su}} \quad (10)$$

The unknown concentration at the surface C_{su} have been assumed to be equal to the concentration in the gas phase C^g . C^g being necessarily superior or equal to C_{su} and each reaction order being over 1, the Weisz-Prater criterion has always been overestimated. Therefore if this overestimated criterion is under the threshold of internal diffusion limitation negligence, no internal diffusion limitations can be assumed.

$$D_e = \frac{\beta_p}{\tau_p} D_M \quad (11)$$

The effective diffusivity estimation is based on the molecular diffusion coefficient (D_M), the particle porosity (β_p) and the particle tortuosity (τ_p). Typical values ($\beta_p=0.6$ and $\tau_p=3$) were considered for the modelling.

The calculated values of the Weisz-Prater criterion have been lowered than 0.3 for every component in all the tested operating conditions. This confirms that internal diffusion limitation can be neglected [19].

3.3 Thermodynamic study

No significant temperature variation was observed along the reactor. This justifies the assumption of isothermicity.

Pure components thermodynamic data have been provided by the DIPPR database or built using Benson method [20] when necessary.

Enthalpies and entropies determined through the Kirch'Hoff equation give access to the Gibbs free energy for each chemical reaction. The equilibrium constants involved in kinetic laws were then calculated as follow:

$$K_{eq} = \exp\left(-\frac{\Delta_r G_T^0}{RT}\right) \left(\frac{P^0}{RT}\right)^{\Delta v} \quad (12)$$

3.4 Reaction scheme

3.4.1 Main pathways

The reactional route (see Figure 2) suggested by Gorin [22] and adapted by Jones et al. [23] is undoubtedly the most accepted mechanism in the literature. This route will therefore be called Gorin-Jones route.

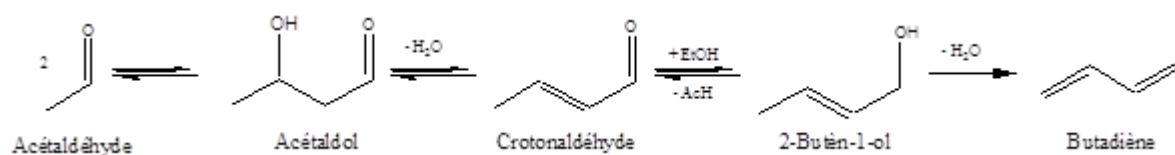


Figure 2 Gorin-Jones route [23]

This route starts with an aldol reaction with rapid loss of H_2O [24]. However there is an additional step where crotonaldehyde turns into 2-buten-1-ol (also called crotyl alcohol) after a redox reaction with EtOH, this latter being transformed into AcH. The last step is the dehydration of 2-buten-1-ol into BD. Generally speaking, these

reactions could be applied to any molecules owning a suitable function (carbonyl or alcohol) which may give a too complex model without lumping some reactions and products for side reactions.

The aldol reaction (addition + condensation) may be considered as reversible [10]. In fact transformation of a mixture of crotonaldehyde and EtOH have been studied over Ta₂O₅-SiO₂ the main products being BD but also AcH [11,23]. The aldol reaction has been established as the rate-limiting step over MgO-SiO₂ over a temperature range of 300 to 400 °C [25].

Meerwein-Ponndorff-Verley reduction (MPV) has been proposed for crotonaldehyde reduction followed by a dehydration to give BD [26,27]. This reaction is also reversible.

The experimental BD/2-buten-1-ol and BD/3-buten-2-ol ratios are far from the ones predicted by the thermodynamic equilibrium. It has then been assumed that the reaction of dehydration of alcohols into olefins are non-reversible in the reaction scheme.

Intramolecular MPV reaction might occur if the molecule has both a carbonyl function and an alcohol. This is the case of acetaldol that might be transformed into 4-hydroxy-butanone (see Figure 3 - i) [28]. After dehydration, this molecule produces methyl vinyl ketone (MVK). MVK has been observed as a side-product in studies of AcH condensation over different catalysts [29]. The intramolecular reaction assumption is reinforced by the presence of AcH in studies of MVK production by acetone/formaldehyde (see Figure 3 - ii) [30].

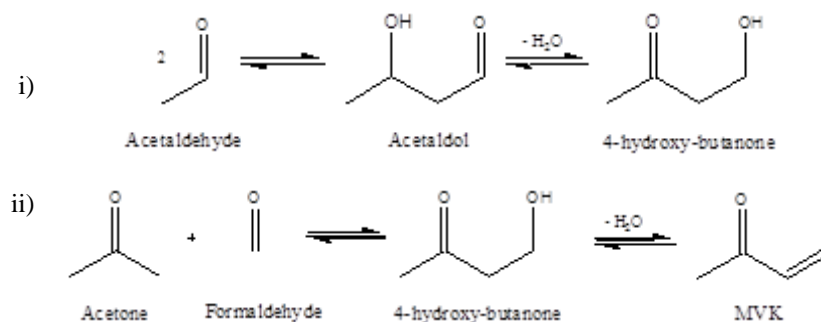


Figure 3 Intra-molecular hydrogen transfer

Moreover Inoue et al. [31] have proved that 4-hydroxy-butanone can be a precursor of BD. Like crotonaldehyde in Gorin-Jones route, MVK can be reduced with an alcohol through MPV reaction into 3-buten-2-ol that can be dehydrated into BD (see Figure 4).

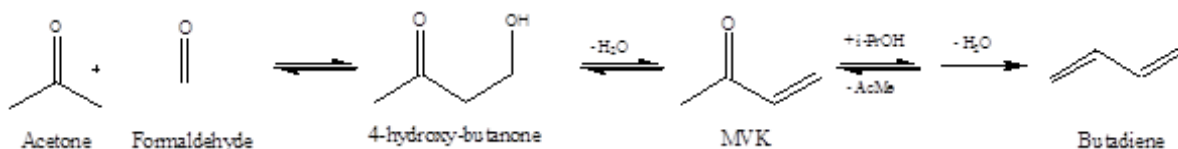


Figure 4 Inoue route [31]

This paper proposes Inoue route for the first time to explain the formation of both butadiene and side products (as seen herein below).

3.4.2 Side reactions

Many side reactions occurs along the assumed main pathways to BD.

Esters formation: Ethyl acetate (EtOAc) is an ester present in the effluent. Esters may be directly formed by Tishchenko reaction or successively by MPV reaction of a hemiacetal produced by the addition of ethanol over acetaldehyde (see Figure 5).

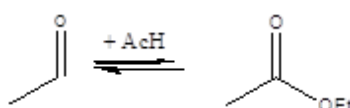


Figure 5 EtOAc formation

A study whose purpose is ethyl acetate recycling pointed out that EtOAc may be part of BD synthesis. Like MPV, this reaction should be considered as reversible [32].

Odd products formation: The experimentally observed [21,23] acetone and formaldehyde may be produced by retroaldol addition of 4-hydroxy-butanone. Both these carbonyl compounds can undergo aldol reaction or MPV reduction permitting the formation of different odd products and producing propylene and pentadienes as final products.

Carbonyls and alcohols C4 formation: Ushikubo and Wada [33] studied the isomerization of 1-butene to 2-butenes of hydrated tantalum oxide at a temperature as low as 100°C. Therefore we may consider that allylic alcohol in the reaction mixture can be isomerized. In this way 2-buten-1-ol may be rearranged into 1-buten-1-ol which is a tautomer of butanal (see Figure 6). In the same way methyl ethyl ketone (MEK) can be produced from

3-buten-2-ol. Such carbonyls can react be reduced by MPV reaction leading to the synthesis of aliphatic alcohols such as butanols.

Olefin and ether formation : As the catalyst can dehydrate 2-buten-1-ol into BD, any alcohol produced can be dehydrated leading to the formation of propene, butene, etc. EtOH is potentially converted directly to ethylene and diethyl ether which are the major by products over tantalum oxide [34,35]. Ethylene formation is favoured at high temperatures on the the contrary of diethyl ether (Et₂O) [36].

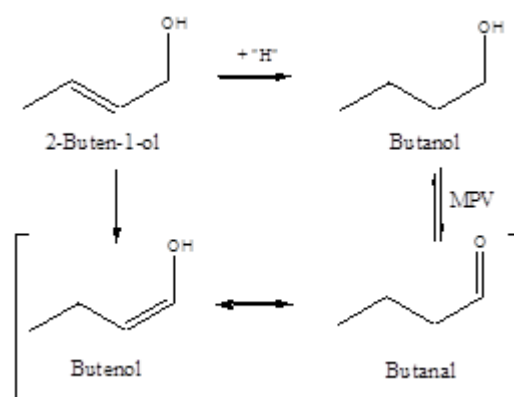


Figure 6 Carbonyl compounds formation

C6+ formation: it has been shown that many heavy compounds are formed in Ostromislensky process conditions [14]. According to Inoue et al. [37], a random polycondensation occurs in the effluent that will lead to heavier products. For the model, these products will be represented by hexatriene, formed after two aldol reaction of AcH, followed by an MPV reaction with EtOH and a dehydration.

3.4.3 Global reaction scheme

Based on the main pathways presented in section 3.4.1 and the side reactions presented in section 3.4.2, a global reaction scheme have been developed (see Figure 7). The reaction scheme takes in account both Gorin-Jones (route a) and Inoue (route b) pathways to BD and pathways to side-molecules.

Acetaldol and 4-hydroxy-butanone (see section 3.4.1) are not observed experimentally. These molecules have therefore been discarded from the model. Acetaldehyde is directly transformed into crotonaldehyde (see reaction 1), MVK (see reaction 2), and acetone (see reaction 3).

Similarly the potential hemiacetal (see section 3.4.2) leading to EtOAc in experimentally unobserved. Therefore the mixture AcH and EtOH is directly transformed into EtOAc (see reaction 13). The pathway presented in this

reaction scheme is the hemiacetal conversion route since it gave better experimental results as latter shown in the discussion.

It has been assumed that the alcohol used for MPV reduction is EtOH since it is in large excess in comparison to other alcohols. Indeed, when EtOH represents at minimum 47 % carbon mass of the effluent (max: 71 %), other alcohols never exceeds 0.4 %.

The purpose of reactions II, III, IV, and V is to emphasize the polycondensation of acetaldehyde while mimicking Gorin-Jones and Inoue pathways. It generates heavy products as observed in the effluent.

Table 1 Global kinetic reaction scheme

| | |
|---|--------------------------|
| 2 AcH ↔ Crotonaldehyde + H₂O | (1a)¹ |
| 2 AcH ↔ MVK + H₂O | (2b)² |
| Crotonaldehyde + EtOH ↔ 2-buten-1-ol + AcH | (3a)³ |
| MVK + EtOH ↔ 3-buten-2-ol + AcH | (3b)³ |
| 2-buten-1-ol → BD + H₂O | (4a)⁴ |
| 3-buten-2-ol → BD + H₂O | (4b)⁴ |
| 2-buten-1-ol ↔ Butanal | (5c)⁵ |
| 3-buten-2-ol ↔ MEK | (5d)⁵ |
| Butanal + EtOH ↔ 1-Butanol + AcH | (6c)³ |
| MEK + EtOH ↔ 2-Butanol + AcH | (6d)³ |
| 1-Butanol → Butene + H₂O | (1c)⁴ |
| 2-Butanol → Butene + H₂O | (1d)⁴ |
| 2 AcH + EtOH ↔ EtOAc + H₂O + EtOH | (7)⁶ |
| 2 AcH ↔ Acetone + Formaldehyde | (8)⁷ |
| Formaldehyde + EtOH → C3 + 2 H₂O | (II)⁸ |
| Acetone + EtOH → C3 + AcH + H₂O | (III)⁹ |
| Acetone + EtOH → C5 + 2 H₂O | (IV)¹⁰ |
| 2 AcH + EtOH → Hexatriene + 3 H₂O | (V)¹¹ |
| EtOH → Ethylene + H₂O | (VI)¹² |
| 2 EtOH ↔ Et₂O + H₂O | (9)¹³ |

↔ : reversible reaction

→ : irreversible reaction

¹aldol reaction; ²aldol reaction + intra-MPV; ³MPV reaction; ⁴dehydration; ⁵isomerisation; ⁶Ester formation; ⁷aldol addition + intra-MPV + retro-aldol; ⁸C3 pathway from Formaldehyde; ⁹C3 pathway from Acetone; ¹⁰C5 pathway; ¹¹C6 pathway; ¹³EtOH dehydration; ¹⁴Et₂O formation

It has been considered that the same type of reactions have the same kinetic parameters. They have therefore been lumped together. The reactions with the same exponent have same kinetic constants and activation energies.

The reactions whose reversibility could not be determined have been considered as reversible by default (isomerisation of butenols into carbonyl compounds).

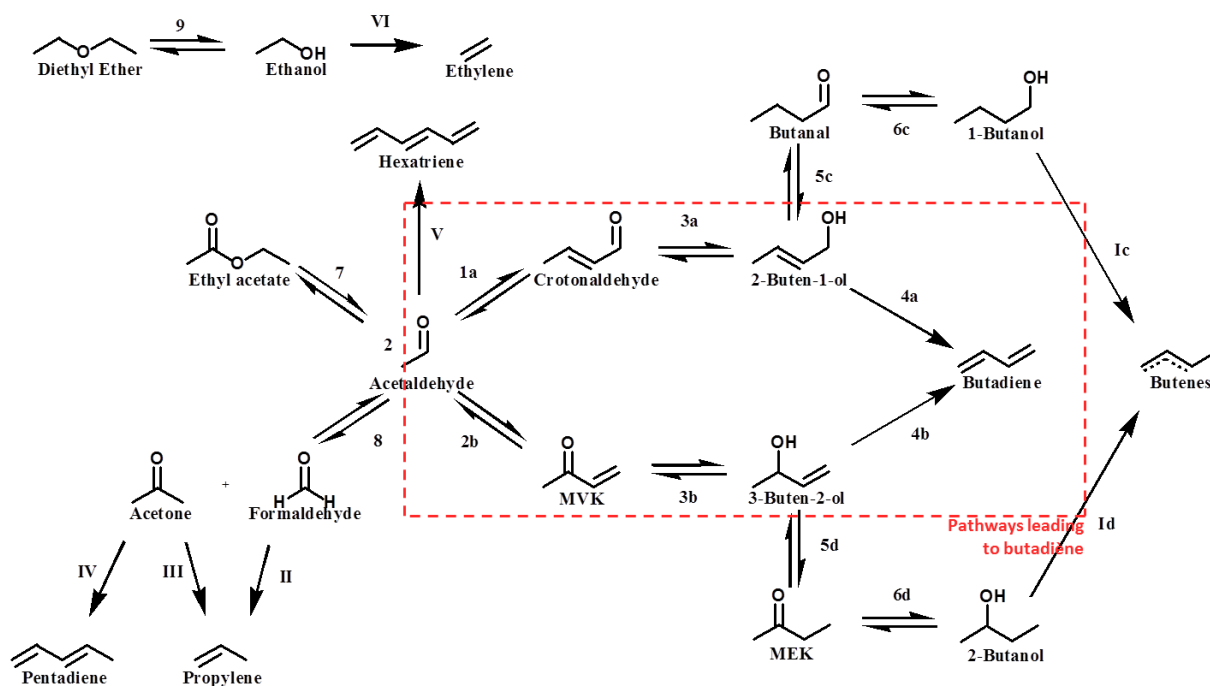


Figure 7 Reaction scheme

Route a : Gorin-Jones route

Route b : Intra-molecular hydrogen route

Route c : butenes formation from 2-buten-1-ol

Route d : butenes formation from 3-buten-2-ol

Arabic numerals : oxygenated compounds and BD formation

Roman numerals : olefins other than BD

4. Results and discussion

4.1 Catalytic results

The experiments have been performed as previously described. The results showed in the following figures (Figure 8 and Figure 9) are given for an EtOH/AcH ratio of 3.6. No carbon mass balance exceeds $\pm 5\%$.

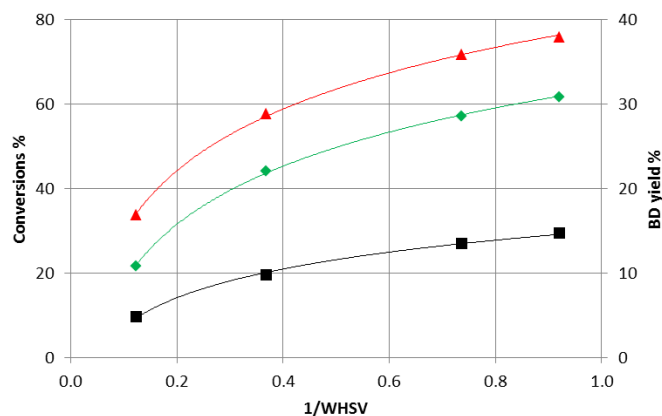


Figure 8 Experimental values at 340 °C and EtOH/AcH ratio of 3.6: EtOH conversion (■), AcH conversion (▲), and BD yield (◆). Lines are drawn to guide the eyes.

The trend of the main components is in accordance with the reaction scheme. Indeed BD yields increases with conversion (see Figure 8). The same trend is observed for the other olefins (C2, C3, C5) for which no conversion was expected. Regarding the heavy products (C6+), the same trend is obtained since their formation is alike to BD production (see supporting information).

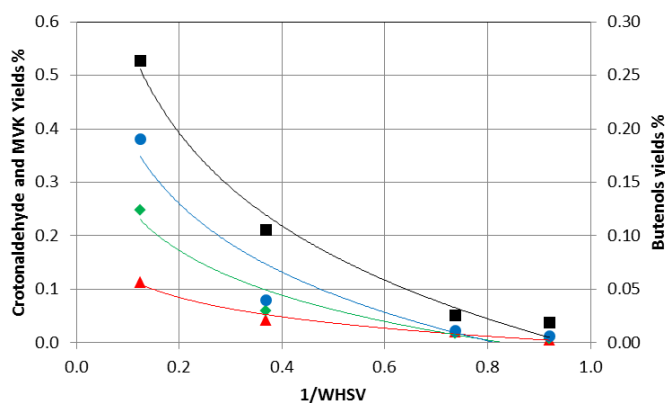


Figure 9 Experimental yields at 340 °C and EtOH/AcH ratio of 3.6: Crotonaldehyde (■), MVK (▲), 2-Buten-1-ol (◆), and 3-Buten-2-ol (●). Lines are drawn to guide the eyes.

Crotonaldehyde, MVK, and butenols yields decrease with increasing conversions (see Figure 9). This is characteristic of intermediates products and in accordance with our reaction scheme. In general, it may be observed that all C3 and C4 oxygenated compounds (EtOAc and diethyl ether excluded) yields decrease with the conversion. This behaviour is characteristic of intermediates products and in accordance with the proposed/assumed reaction scheme.

The main side products are ethylene, Et₂O, and EtOAc (see yields in supporting information).

4.2 Kinetic approach

The kinetic model relies on the reaction scheme presented in Table 1 and associated order-based kinetic laws.

Those are defined as follow (see equation (13)).

$$r = k \left(\prod C_{reactants}^{v_{reactants}} - \frac{1}{K_{eq}} \prod C_{products}^{v_{products}} \right) \quad (13)$$

The kinetic constants are based on Arrhenius law (see equation (14)).

$$k = k^{\circ} * \exp \left[-\frac{E_a}{R} \left(\frac{1}{T_{ref}} - \frac{1}{T} \right) \right] \quad (14)$$

With the temperature of reference $T_{ref} = 340^{\circ}\text{C}$

The same pre-exponential factors and activation energies have been assigned to the same type of reactions.

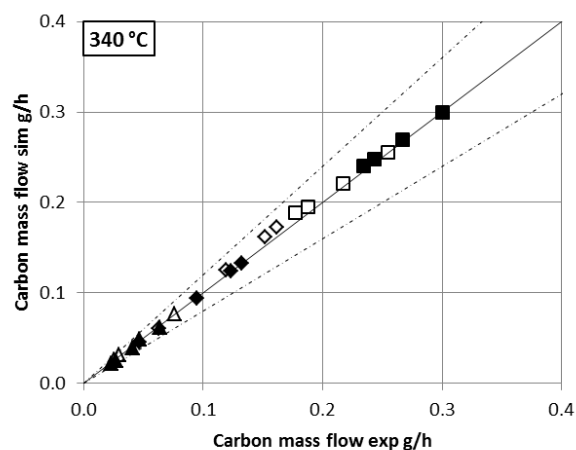
Kinetic parameter estimation was achieved by fitting calculated and experimental carbon mass flow for each component. Experimental data at constant temperature were used to first estimate pre-exponential factors. Activation energies were then assessed through experimental data at different temperatures. The estimated values of pre-exponential factors and activation energies are reported in Table 2 and Table 3.

Table 2 Estimated pre-exponential factors at 340 °C

| Reaction exponent | Reaction type | $k^{\circ} \times 10^3$ | Units |
|-------------------|---|-------------------------|---|
| 1 | <i>Aldol reaction</i> | 0.3 | $(\text{m}^3)^2 \cdot \text{kg}_{\text{cata}}^{-1} \cdot \text{mol}^{-1} \cdot \text{s}^{-1}$ |
| 2 | <i>Aldol reaction + intra-MPV</i> | 6.4×10^{-2} | $(\text{m}^3)^2 \cdot \text{kg}_{\text{cata}}^{-1} \cdot \text{mol}^{-1} \cdot \text{s}^{-1}$ |
| 3 | <i>MPV reaction</i> | 36 | $(\text{m}^3)^2 \cdot \text{kg}_{\text{cata}}^{-1} \cdot \text{mol}^{-1} \cdot \text{s}^{-1}$ |
| 4 | <i>Dehydration</i> | 9.4 | $\text{m}^3 \cdot \text{kg}_{\text{cata}}^{-1} \cdot \text{s}^{-1}$ |
| 5 | <i>Isomerisation</i> | 0.14 | $\text{m}^3 \cdot \text{kg}_{\text{cata}}^{-1} \cdot \text{s}^{-1}$ |
| 6 | <i>Ester formation</i> | 3.6×10^{-4} | $(\text{m}^3)^2 \cdot \text{kg}_{\text{cata}}^{-1} \cdot \text{mol}^{-1} \cdot \text{s}^{-1}$ |
| 7 | <i>aldol addition + intra-MPV + retro-aldol</i> | 4.5×10^{-3} | $(\text{m}^3)^2 \cdot \text{kg}_{\text{cata}}^{-1} \cdot \text{mol}^{-1} \cdot \text{s}^{-1}$ |
| 8 | <i>C3 pathway from Acetone</i> | 0.65 | $(\text{m}^3)^2 \cdot \text{kg}_{\text{cata}}^{-1} \cdot \text{mol}^{-1} \cdot \text{s}^{-1}$ |
| 9 | <i>C3 pathway from Formaldehyde</i> | 5.4×10^{-3} | $(\text{m}^3)^3 \cdot \text{kg}_{\text{cata}}^{-1} \cdot \text{mol}^{-2} \cdot \text{s}^{-1}$ |
| 10 | <i>C5 pathway</i> | 0.54 | $(\text{m}^3)^2 \cdot \text{kg}_{\text{cata}}^{-1} \cdot \text{mol}^{-1} \cdot \text{s}^{-1}$ |
| 12 | <i>C6 pathway</i> | 5.0×10^{-4} | $(\text{m}^3)^3 \cdot \text{kg}_{\text{cata}}^{-1} \cdot \text{mol}^{-2} \cdot \text{s}^{-1}$ |
| 13 | <i>EtOH dehydration</i> | 8.0×10^{-3} | $\text{m}^3 \cdot \text{kg}_{\text{cata}}^{-1} \cdot \text{s}^{-1}$ |
| 14 | <i>Et₂O formation</i> | 4.4×10^{-4} | $(\text{m}^3)^2 \cdot \text{kg}_{\text{cata}}^{-1} \cdot \text{mol}^{-1} \cdot \text{s}^{-1}$ |

4.2.1 Parity and flow diagrams

A parity diagram showing simulated EtOH, AcH and BD carbon mass flows for both EtOH/AcH ratio at 340 °C is represented in Figure 10. The simulated EtOH, AcH, and BD carbon mass flows show very good agreement between experimental and simulated values for both ratios. This model is therefore very accurate in order to model the main components of the effluent.



**Figure 10 Parity diagramm for different WHSV: EtOH (■), AcH (▲), BD (◆).
EtOH/AcH ratio: 3.6 (full symbols) ; 2.5 (empty symbols). T: 340 °C**

The intermediates to be considered for BD formation are crotonaldehyde, MVK, 2-buten-1-ol, and 3-buten-2-ol. Simulated and experimental carbon mass flows of these molecules are represented in Figure 11 (carbonyl compounds) and Figure 12 (butenols). The simulated crotonaldehyde and MVK carbon mass flows are in very good agreement between experimental and calculated values for both ratios. In the case of 2-buten-1-ol and 3-buten-2-ol, even if simulated values follow the experimental trend, significant discrepancies are observed. However, this is sufficient to assess the validity of the model if we take into account that it is very difficult to fit over very low concentrated compounds.

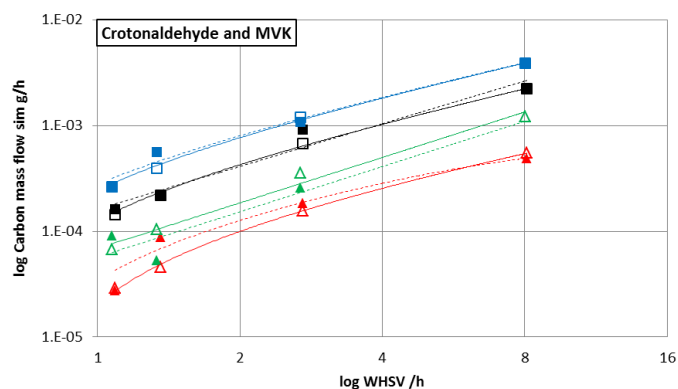


Figure 11 Experimental (solid symbols) and simulated (open symbols) values of intermediates carbon mass flows: Crotonaldehyde (■), MVK (▲). EtOH/AcH ratio: 3.6 (black and red) ; 2.5 (blue and green). T: 340 °C. Lines are drawn to guide the eyes.

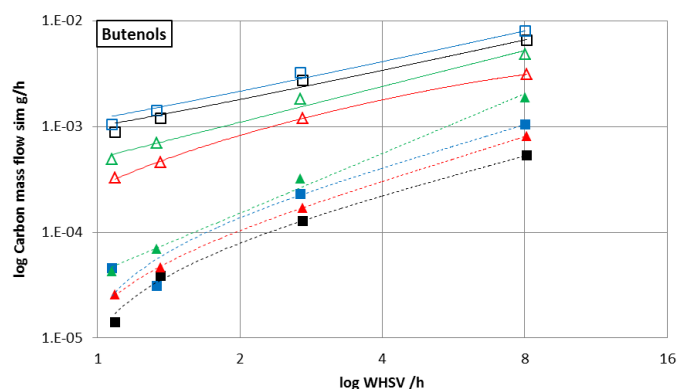


Figure 12 Experimental (solid symbols) and simulated (open symbols) values of intermediates carbon mass flows: 2-Buten-1-ol (■), 3-Buten-2-ol (▲). EtOH/AcH ratio: 3.6 (black and red) ; 2.5 (blue and green). T: 340 °C. Lines are drawn to guide the eyes.

Inoue route has to be taken in account for some side products formation *i.e.* 3-buten-2-ol (see Figure 3) and MVK, a proven source of BD [31], well fitted here for both ratios (see Figure 11). This reaction route allows to explain the presence of MEK, 2-butanol and compounds with an odd carbon number such as acetone, propylene, pentadiene (see Figure 4 and supporting information). This compounds presence cannot be explained through the traditionnal Gorin-Jones route.

Regarding the butadiene formation scheme, acetaldehyde conversion leading to BD production, *i.e.* aldol reaction (1a) and {aldol + intra MPV} reaction (2b), appears to be the rate limiting reaction for Gorin Jones and Inoue routes respectively. In fact the pre exponential factor of aldol reaction (1a) is less than 5 times higher than the one of {aldol + intra MPV} reaction (1b) (see Table 2). As a consequence aldol reaction rate (1a) is between

1.5 and 3.7 times faster than {aldol + intra MPV} reaction (2b) rate, indicating that Gorin Jones route is not significantly faster than Inoue route. From this rate considerations, BD production from Inoue route represents from about 20 to 40 % of BD total production (see supporting information). The model indicates therefore that, over Ta₂O₅-SiO₂, Gorin Jones route is the main contribution route for BD production but also that Inoue route has to be taken in account for both side-products and BD production.

Concerning the main side products (ethylene, Et₂O, and EtOAc) comparison of simulated and experimental carbon mass flows are presented in Figure 13. The simulated values fit the experimental values within the range of ± 20 % for both ratios. Indeed these compounds are apart from the main reactional pathway and one can assess that they are easier to model because they do not depend on other reactions. Two pathways had been proposed to explain EtOAc formation: via hemiacetal conversion and Tishchenko reaction. Using the latter reaction, EtOAc carbon flows cannot be properly simulated since the error is outside of the range. This reaction has thus been discarded in favour of hemiacetal conversion.

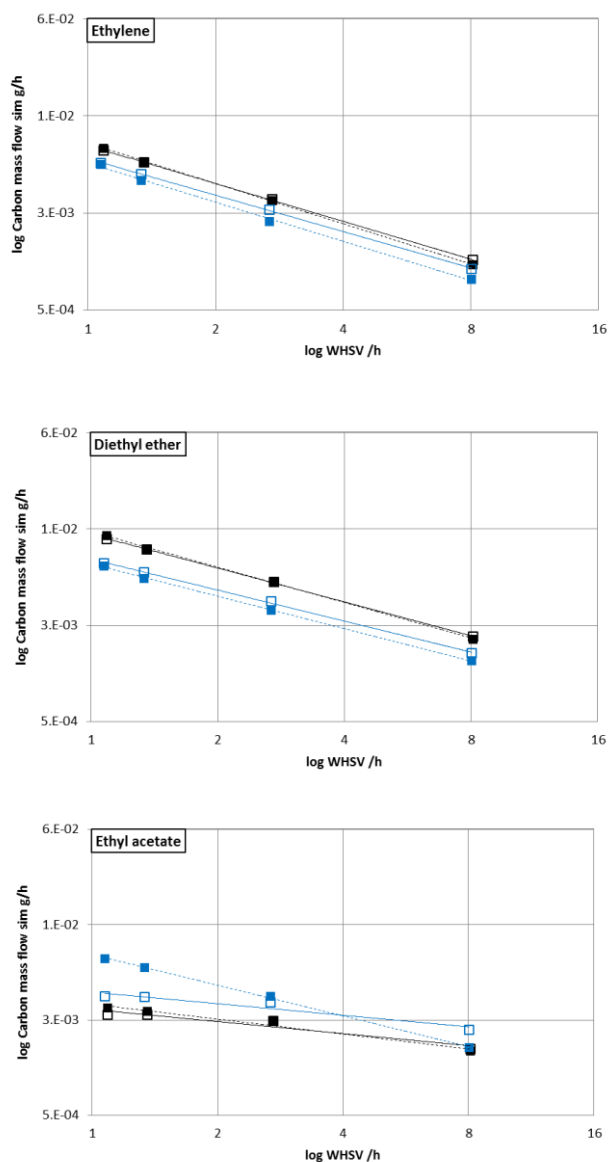


Figure 13 Experimental (solid symbols) and simulated (open symbols) carbon mass flows. EtOH/AcH ratio: 3.6 (black) ; 2.5 (blue). T: 340 °C. Lines are drawn to guide the eyes.

Olefins with odd carbon numbers (C3 and C5) are side-products produced from Inoue pathway. Propylene calculated carbon mass flows respect the 20 % margin for both ratios. Pentadiene carbon mass flows present also very good agreement except for the highest WHSV.

Other side products, *i.e.* butenes, minor oxygenated C4 and heavy products, experimental carbon mass flows cannot be suitably represented. Indeed, even if the order of magnitude of simulated and experimental carbon mass flows of butenes are similar, the general evolution with WHSV is not respected. Regarding the other oxygenated C4: MEK, butanal and butanols, the simulated carbon mass flows were significantly underestimated.

For those compounds, considering another consumption pathway may be necessary to match experimental values.

In overall, the molecules concentrations well represented by the model at 340 °C represent 97 to 98 % of the effluent, validating the relevance of our reaction scheme and the chosen kinetic approach.

4.2.2 Activation energies

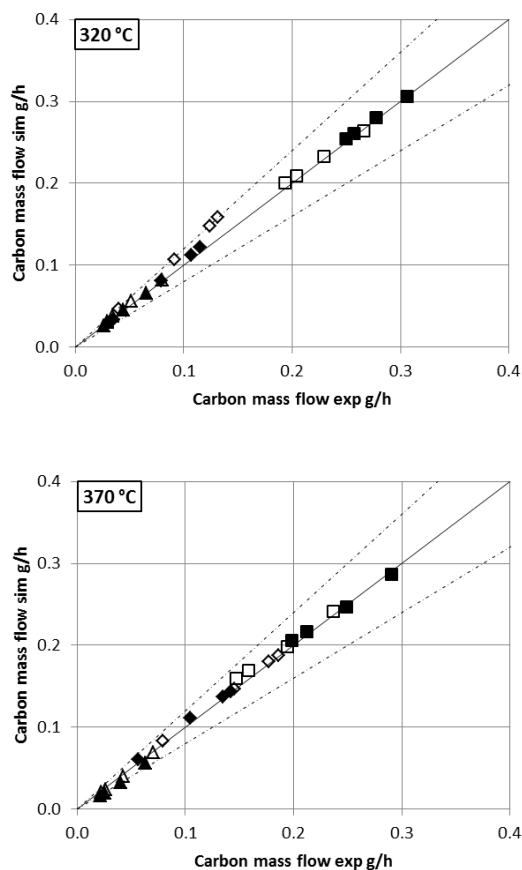
The activation energies have been estimated from 320 °C to 370 °C. Table 3 contains only estimated activation energies reactions and not all reactions. The estimations were made for intermediates and main side-products. Since the minor side products activation energies could not yield reliable results, they were arbitrary set to 50 kJ/mol.

Table 3 Estimated activation energies

| Exponent | Reaction type | E_a (kJ/mol) |
|-----------------|---------------------------------------|-------------------------------|
| 1 | <i>Aldol reaction</i> | 40 |
| 2 | <i>Aldol reaction + intra-MPV</i> | 40 |
| 3 | <i>MPV reaction</i> | 45 |
| 4 | <i>Dehydration</i> | 55 |
| 6 | <i>Ester formation</i> | 41 |
| 13 | <i>EtOH dehydration</i> | 157 |
| 14 | <i>Et₂O formation</i> | 103 |

Few kinetic studies with tantalum based catalyst can be found in the litterature in order to make a relevant comparison of the different reaction activation energies over the same catalyst. For example Legendre and Cornet [38] obtain very different values for the dehydration of EtOH (84 kJ/mol) and its condensation into Et₂O (88 kJ/mol) over Ta₂O₅. Balandin et al. [39] obtains nearly the same value for iso-propanol dehydration (99 kJ/mol) also over non supported tantalum oxide. The calculated values in this study are very different over Ta₂O₅-SiO₂ (see Table 3) but ethylene and Et₂O carbon mass flows are very well respected in all our results. Indeed all values but one respect the 20 % margin of error, which makes trustable the reaction activation energies estimated in this work.

The relative difference between simulated and experimental carbon mass flows does not exceed ± 20 % for the main components (*i.e.* EtOH, AcH, and BD) for all EtOH/AcH ratios and temperatures (see Figure 14). This confirms the relevance of the assumed reaction scheme and related kinetic laws.



**Figure 14 Parity diagramm for different WHSV: EtOH (■), AcH (▲), BD (◆).
EtOH/AcH ratio: 3.6 (full symbols) ; 2.5 (empty symbols). T: 320 °C and 370 °C**

Inoue et al. [37] obtained a very similar activation energy for the aldol reaction (45 kJ/mol) with a equivalent catalyst. Nevertheless, the representation of the intermediates carbon mass flows is not satisfactory at both 320 °C and 370 °C. The difficulty of estimating activation energies in this work is related to their low impact on the calculated flow composition. Indeed a variation of 20 % of the activation energies induces only a variation of 5, 6 an 6 % maximum for EtOH, AcH, and BD carbon mass flows respectively to the simulated carbon mass flows obtained with the estimated activation energies. The temperature range should be increase and the model be upgraded to obtain more reliable estimations of activation energies.

5. Conclusion

A global reaction scheme for the formation of BD from an EtOH/AcH mixture was built based on a literature review. This reaction scheme consists of two pathways : Gorin-Jones pathway, widely accepted in the litterature, and a route involving intra-molecular hydrogen, that implicates respectively crotonaldehyde and MVK as

intermediate: Inoue route. Additional side reactions have to be taken into account to accurately represent effluent composition through the formation of major (ethylene, Et₂O and EtOAc) and minor (other olefins, C₄ oxygenated and heavy compounds) side products. Order-based kinetic laws were implemented in the model for each chemical reaction. The experimental values have been acquired over a temperature range of 320 °C to 370 °C, with two EtOH/AcH ratios (3.6 and 2.5) and a WHSV range of 1.1 to 8 g g_{cata}⁻¹ h⁻¹.

The simulated carbon mass flows of the carbonyl intermediates of the BD pathway were in good agreement with the experimental values for both EtOH/AcH ratios and all WHSV at 340 °C. The butenols were the only intermediates showing significant discrepancies between experimental and simulated values even if the experimental trends is reproduced.

These results show that, unlike generally assumed in the literature, intra-molecular hydrogen transfer pathway has to be taken into account to accurately predict the presence of many side products.

The simulated carbon mass flows of the main side products (*i.e.* ethylene, ethyl ether, and ethyl acetate) were in good agreement with experimental values at 340 °C. Nevertheless, the unaccurate representation of some other side products indicates that the model still has to be improved. This fact may be the consequence of some side reactions and reaction kinetic constants lumps.

This kinetic model is already satisfactory since accurately reproducing main components of the effluent for all operatory conditions tested. While this model needs to be improved to accurately represent all side products, this kinetic study already indicates that Inoue pathway has to be added along Gorin-Jones pathway to explain the transformation of EtOH/AcH into BD.

References

- [1] J.A. Posada, A.D. Patel, A. Roes, K. Blok, A.P.C. Faaij, M.K. Patel, Potential of bioethanol as a chemical building block for biorefineries: preliminary sustainability assessment of 12 bioethanol-based products, *Bioresour. Technol.* 135 (2013) 490-499. <https://doi.org/10.1016/j.biortech.2012.09.058>
- [2] W.C. White, Butadiene production process overview, *Chem.-Biol. Interact.* 166 (2007) 10-14. <https://doi.org/10.1016/j.cbi.2007.01.009>
- [3] A.D. Patel, K. Meesters, H. den Uil, E. de Jong, K. Blok, M.K. Patel, Sustainability assessment of novel chemical processes at early stage, *Energy Environ. Sci.* 5 (2012) 8430-8444. <https://doi.org/10.1039/C2EE21581K>

- [4] G.O. Ezinkwo, V.P. Tretyakov, A. Aliyu, A.M. Ilolov, Fundamental Issues of Catalytic Conversion of Bio-Ethanol into Butadiene, *ChemBioEng Rev.* 1 (2014) 194-203. <https://doi.org/10.1002/cben.201400007>
- [5] E.V. Makshina, M. Dusselier, W. Janssens, J. Degreève, P.A. Jacobs, B.F. Sels, Review of old chemistry and new catalytic advances in the on-purpose synthesis of butadiene, *Chem. Soc. Rev.* 43 (2014) 7917-7953. <https://doi.org/10.1039/C4CS00105B>
- [6] J. Sun and Y. Wang, Recent Advances in Catalytic Conversion of Ethanol to Chemicals, *ACS Catal.* 4 (2014) 1078-1090. <https://doi.org/10.1021/cs4011343>
- [7] J. Ostromislenky, *J. Russ. Phys.-Chem. Soc.* 47 (1915) 1472.
- [8] V.L. Sushkevich, I.I. Ivanova, V.V. Ordonsky, E. Taarning, Design of a metal-promoted oxide catalyst for the selective synthesis of butadiene from ethanol, *ChemSusChem* 7 (2014) 2527-2536. <https://doi.org/10.1002/cssc.201402346>
- [9] B.B. Corson, H.E. Jones, C.E. Welling, J.A. Hinckley, E.E. Stahly, Butadiene from ethyl alcohol - Catalysis in the one- and two-step processes, *Ind. Eng. Chem.* 42 (1950) 359-373. <https://pubs.acs.org/doi/pdf/10.1021/ie50482a039>
- [10] W.J. Toussaint, J.T. Dunn, D.R. Jackson, Production of butadiene from alcohol, *Ind. Eng. Chem.* 39 (1947) 120-125. <https://pubs.acs.org/doi/pdf/10.1021/ie50446a010>
- [11] W.M. Quattlebaum, W.J. Toussaint, J.T. Dunn, Deoxygenation of Certain Aldehydes and Ketones: Preparation of Butadiene and Styrene, *J. Am. Chem. Soc.* 69 (1947) 593-599. <https://pubs.acs.org/doi/pdf/10.1021/ja01195a040>
- [12] B.B. Corson, E.E. Stahly, H.E. Jones, H.D. Bishop, Butadiene from Ethyl Alcohol - Study of the variables of operation, *Ind. Eng. Chem.* 41 (1949) 1012-1017. <https://pubs.acs.org/doi/pdf/10.1021/ie50473a028>
- [13] Q. Zhu, B. Wang, T. Tan, Conversion of Ethanol and Acetaldehyde to Butadiene over MgO–SiO₂ Catalysts: Effect of Reaction Parameters and Interaction between MgO and SiO₂ on Catalytic Performance, *ACS Sustainable Chem. Eng.* 5 (2017) 722-733. <https://doi.org/10.1021/acssuschemeng.6b02060>
- [14] H.-J. Chae, T.-W. Kim, Y.-K. Moon, H.-K. Kim, K.-E. Jeong, C.-U. Kim, S.-Y. Jeong, Butadiene production from bioethanol and acetaldehyde over tantalum oxide-supported ordered mesoporous silica catalysts, *Appl. Catal., B* 150 (2014) 596-604. <https://doi.org/10.1016/j.apcatb.2013.12.023>
- [15] T.-W. Kim, J.-W. Kim, S.-Y. Kim, H.-J. Chae, J.-R. Kim, S.-Y. Jeong, C.-U. Kim, Butadiene production from bioethanol and acetaldehyde over tantalum oxide-supported spherical silica catalysts for circulating fluidized bed, *Chem. Eng. J.* 278 (2015) 217-223. <https://doi.org/10.1016/j.cej.2014.09.110>

- [16] C. Angelici, B.M. Weckhuysen, P.C.A. Bruijninx, Chemocatalytic conversion of ethanol into butadiene and other bulk chemicals, *ChemSusChem* 6 (2013) 1595-1614. <https://doi.org/10.1002/cssc.201300214>
- [17] A.-V. Brosteanu, I. Banu, G. Bozga, Recent Progresses in Ethanol Conversion to 1,4-Butadiene, *Bull. Rom. Chem. Eng. Soc.* 5 (2018) 1-106. http://sicer.ro/wp-content/uploads/2019/02/BRChES_vol.5_no.1_2018.pdf#page=4
- [18] K. Radhakrishnan and A.C. Hindmarsh, Description and use of LSODE, the Livermore Solver for Ordinary Differential Equations, Technical Report NASA-RP-1327, E-5843, NAS 1.61:1327, UCRL-ID-113855 (1993). <https://ntrs.nasa.gov/archive/nasa/casi.ntrs.nasa.gov/19940030753.pdf>
- [19] D. Schweich, Génie de la réaction chimique, Tech&Doc, Paris, 2001.
- [20] E.B. Poling, J.M. Prausnitz, J.P. O'Connell, *The Properties of Gases and Liquids*, fifth ed., McGraw-Hill, 2001.
- [21] P.B. Weisz and C.D. Prater, Interpretation of Measurements in Experimental Catalysis, *Adv. Catal.* 6 (1954) 143-196. [https://doi.org/10.1016/S0360-0564\(08\)60390-9](https://doi.org/10.1016/S0360-0564(08)60390-9)
- [22] Y.A. Gorin, Catalytic conversions of alcohols into bivinyl hydrocarbons. XV. General laws of formation of diethylenic hydrocarbons with a conjugate bond system, *Russ. J. Gen. Chem.* 19 (1949) 877-883.
- [23] H.E. Jones, E.E. Stahly, B.B. Corson, Butadiene from alcohol. Reaction mechanism, *J. Am. Chem. Soc.* 71 (1949) 1822-1828. <https://pubs.acs.org/doi/pdf/10.1021/ja01173a084>
- [24] C.R. Ho, S. Shylesh, A.T. Bell, Mechanism and Kinetics of Ethanol Coupling to Butanol over Hydroxyapatite, *ACS Catal.* 6 (2016) 939-948. <https://doi.org/10.1021/acscatal.5b02672>
- [25] S. Da Ros, M.D. Jones, D. Mattia, M. Schwaab, E. Barbosa-Coutinho, R.C. Rabelo-Neto, F. Bellot Noronha, J.C. Pintoa, Microkinetic analysis of ethanol to 1,3-butadiene reactions over MgO-SiO₂ catalysts based on characterization of experimental fluctuations, *Chem. Eng. J.* 308 (2017) 988-1000. <https://doi.org/10.1016/j.cej.2016.09.135>
- [26] S. Kvisle, A. Agüero, R.P.A. Sneed, Transformation of ethanol into 1,3-butadiene over magnesium oxide/silica catalysts, *Appl. Catal.* 43 (1988) 117-131. [https://doi.org/10.1016/S0166-9834\(00\)80905-7](https://doi.org/10.1016/S0166-9834(00)80905-7)
- [27] H. Niiyama, S. Morii, E. Echigoya, Butadiene from ethanol over Silica-magnesium catalysts, *Bull. Chem. Soc. Jpn.* 45 (1972) 655-659. <https://doi.org/10.1246/bcsj.45.655>
- [28] M. Gines and E. Iglesia, Bifunctional condensation reactions of alcohols on basic oxides modified by copper and potassium, *J. Catal.* 176 (1998) 155-172, 1998. <https://doi.org/10.1006/jcat.1998.2009>

- [29] V.V. Ordonsky, V.L. Sushkevich, I.I. Ivanova, Study of acetaldehyde condensation chemistry over magnesia and zirconia supported on silica, *J. Mol. Catal. A-Chem.* 333 (2010) 85-93. <https://doi.org/10.1016/j.molcata.2010.10.001>
- [30] M. Ai, The Production of Methyl Vinyl Ketone by the Vapor-Phase Aldol Condensation between Formaldehyde and Acetone, *J. Catal.* 106 (1987) 273-279. [https://doi.org/10.1016/0021-9517\(87\)90231-4](https://doi.org/10.1016/0021-9517(87)90231-4)
- [31] R. Inoue, A. Ichikawa, K. Furukawa, Synthesis of Butadiene from 4-oxy-2-butanone and alcohol, *J. Chem. Soc. Jpn.* 61 (1958) 566-569.
- [32] E.E. Stahly, H.E. Jones, B. B. Corson, Butadiene from ethanol, *Ind. Eng. Chem.* 40 (1948) 2301-2303. <https://pubs.acs.org/doi/pdf/10.1021/ie50468a017>
- [33] T. Ushikubo and K. Wada, Catalytic properties of hydrated tantalum oxide, *Appl. Catal.* 67 (1990) 25-38. [https://doi.org/10.1016/S0166-9834\(00\)84429-2](https://doi.org/10.1016/S0166-9834(00)84429-2)
- [34] R. Inoue, A. Ichikawa, K. Furukawa, The yield of Butadiene from Ethyl alcohol and Acetaldehyde, *Kobunshi Kagaku* 15 (1958) 136-142.
- [35] P.I. Kyriienko, O.V. Larina, S.O. Soloviev, S.M. Orlyk, S. Dzwigaj, High selectivity of TaSiBEA zeolite catalysts in 1,3-butadiene production from ethanol and acetaldehyde, *Catal. Commun.* 77 (2016) 123-126. <https://doi.org/10.1016/j.catcom.2016.01.023>
- [36] R. Inoue, A. Ichikawa, K. Furukawa, Reaction of Ethyl alcohol on Ta₂O₅-SiO₂ gel catalyst, *J. Chem. Soc. Jpn.* 60 (1957) 37-40.
- [37] R. Inoue, A. Ichikawa, K. Furukawa, Polycondensation of acetaldehyde, *Kobunshi Kagaku* 14 (1957) 277-282.
- [38] M. Legendre and D. Cornet, Catalytic oxidation of Ethanol over Tantalum oxide, *J. Catal.* 25 (1972) 194-203. [https://doi.org/10.1016/0021-9517\(72\)90218-7](https://doi.org/10.1016/0021-9517(72)90218-7)
- [39] A.A. Balandin, N.P. Sokolova, Y.P. Simanov, The Pentoxides of Niobium and Tantalum as Dehydration Catalysts, *Russ. Chem. Bull.* 10 (1961) 383-391. <https://doi.org/10.1007/BF01131052>